
Multi-Spacecraft Attitude Path Planning Using Consensus with LMI-Based Exclusion Constraints

Innocent Okoloko

Additional information is available at the end of the chapter

<http://dx.doi.org/10.5772/intechopen.71580>

Abstract

Space missions involving multi-vehicle teams require the cooperative navigation and attitude slewing of the spacecraft or satellites, for such purposes as interferometry and optimal sensor coverage. This introduces extra constraints of exclusion zones between the spacecraft, in addition to the default exclusion constraints already introduced by damaging or blinding celestial objects. In this work, we present a quaternion-based attitude consensus protocol by using the communication topology of the spacecraft team. By using the Laplacian matrix of their communication graph and a semidefinite program, a synthesis of a time-varying optimal stochastic matrix P is done, which is used to generate various consensus and cooperative attitude trajectories from the initial attitudes of the spacecraft. The concept of quaternion-based quadratically constrained attitude control is then employed to satisfy cone avoidance constraints, where exclusion zones are identified, expressed as linear matrix inequalities (LMI), and solved by semidefinite programming (SDP).

Keywords: attitude path planning, consensus, exclusion, optimization, LMI

1. Introduction

Attitude control is the process of making a spacecraft, e.g. a satellite to point toward a specific direction of interest, and attitude path planning is an essential part of space missions. Some current and future space missions require the deployment of teams of spacecraft for such purposes as interferometry and sensor coverage, e.g. [1, 2]. The general problem of attitude control (AC) is important, not only in the navigation of satellites but also of other spacecraft [3], aircraft, and robots. For this reason, the topic has been studied extensively in the literature, e.g. [4–10].

Attitude path planning is a challenging problem and becomes more challenging when it involves multiple spacecraft. First, they are moving at very high speed in highly dynamic

Notation	Meaning
SC_i, SC_i	Spacecraft i
q^i	Attitude quaternion vector of $SC_i, SC_i, q^i = [q_1 \ q_2 \ q_3 \ q_4]^T$
q^{-i} or q^i	Conjugate of q^i
\bar{q}^i	Vector part of $q^i, \bar{q}^i = [q_1 \ q_2 \ q_3]^T$
$\bar{q}^{i \times}$	Antisymmetric of q^i
\mathbf{q}	Stacked vector of more than one quaternion vectors
\mathbf{q}^{off}	Stacked vector of more than one offset quaternion vectors
Ω, Π	Quaternion dynamics plant matrix
\mathbf{P}	Quaternion dynamics Laplacian-like plant matrix
ω	Angular velocity
τ	Control torque
J	Inertia matrix
\mathbf{L}	Laplacian matrix
\mathbf{P}	Laplacian-like stochastic matrix
\mathbf{I}_n	Then $n \times n$ identity matrix
\mathcal{S}^m	The set of $m \times m$ positive definite matrices
\bar{A}	Cone avoidance constraint matrix
\mathcal{R}^i	Rotation matrix corresponding to q^i
$\mathcal{F}_{SC_i}^I$	Fixed coordinate (Inertial) frame with origin at SC_i 's center
$\mathcal{F}_{SC_i}^B$	Rotational coordinate (Body) frame with origin at SC_i 's center
$v_{obs_i}^B$	Vector of obstacle in $\mathcal{F}_{SC_i}^B$
$v_{obs_i}^I$	Vector of obstacle in $\mathcal{F}_{SC_i}^I$
$v_{obs_i, j}^I$	Vector of the j^{th} obstacle in $\mathcal{F}_{SC_i}^I$
$v_{cam_i}^B$	Vector of the SC_i 's camera in $\mathcal{F}_{SC_i}^B$
$v_{cam_i}^I$	Vector of the SC_i 's camera in $\mathcal{F}_{SC_i}^I$
\otimes	Kronecker multiplication operator
\odot	Quaternion multiplication operator
\ominus	Quaternion difference operator
t_0	Initial time
t_f	Final time
x^i	Position vector of SC_i, SC_i
\mathbf{x}	Stacked vector of n position vectors
$(x^{ij})^{off}$	Offset vector between i and j
\mathbf{x}^{off}	Stacked vector of n offset vectors
\mathcal{C}	The consensus space for $\mathbf{q}, \mathcal{C} = \{\mathbf{q} q^1 = q^2 = \dots = q^n\}$

Table 1. Frequently used notations in this chapter.

environments, subject to external constraints such as blinding celestial objects, which can damage onboard sensors. Secondly, because they are in a team, they must be careful with each other when changing attitude, so as not to collide with each other and damage appendages. We consider a team of networked spacecraft, which share some common objectives, where consensus theory based on graph Laplacians can be applied [11, 12].

Spacecraft attitude dynamics is usually represented by unit quaternions because quaternion dynamics do not encounter the singularities associated with other representations. However, quaternion dynamics are non-linear, which makes it difficult to apply Laplacian-like dynamics directly to quaternions.

Next, we consider some previous work on constrained attitude path planning. In [4], attitude control was formulated as a quadratically constrained optimization problem. Linear matrix inequalities (LMIs) and semidefinite programming (SDP) were employed to solve it for a multiple spacecraft scenario in [6]. In [10], spacecraft attitude stabilization on a sphere was studied. The control torques required for effective attitude stabilization were reduced from three to two. In [12], a consensus-based approach was applied in distributed attitude alignment of a team of communicating spacecraft flying in formation. In [13], a Laplacian-based protocol implemented using the *modified Rodriguez parameters* (MRP) was employed in *leader following* attitude control of spacecraft.

However, none of these aforementioned works apply consensus theory directly to quaternions, except our previous works [7–9]. In addition, only [4, 6–9] tackle the important problem of attitude cone avoidance constraints. Moreover, the works [4, 6, 7] were developed for spacecraft in the same coordinate frame, which does not have a direct practical implementation unless developed further.

To handle the difficulty of nonlinearity in quaternion kinematics, we cast the Q-CAC problem as a semidefinite program, which is subject to convex quadratic constraints, stated as LMI. Then a series of Laplacian-like matrices are synthesized, which satisfy the constraints and enables the spacecraft achieve consensus with exclusion. We employed available optimization software tools such as Sedumi [14] and Yalmip [15] running inside MATLAB[®], for simulation.

Moreover, the solution presented here was developed for the realistic scenario of spacecraft in different coordinate frames, making it practical to implement directly. Therefore, the contributions of this chapter are aspects of our previous works [7–9], which are: (1) development of a quaternion consensus protocol; (2) incorporating dynamic cone avoidance constraints into the consensus framework; (3) providing a mathematical convergence analysis for the quaternion-based consensus framework; (4) extending the approach to multiple spacecraft in any coordinate frames, thereby making it more suitable for practical implementation.

The rest of the chapter is organized as follows: The problem statement is in Section 2, followed by brief mathematical preliminaries in Section 3. The solution technique and convergence analysis are in Section 4, numerical simulations in Section 5, and conclusion in Section 6. Notations frequently used in this chapter are listed in **Table 1**. The words *obstacle*, *avoidance*, *exclusion*, *exclusion vector* may be used interchangeably in this chapter.

2. Problem statement

The problem of attitude reconfiguration of a team of communicating spacecraft with avoidance constraints can be stated as follows. Given a set of communicating spacecraft with initial positions at $x^i(t_0) \in \mathbb{R}^3$ $i=1 \dots n$, initial attitudes represented by quaternions $q^i(t_0)$, generate a sequence of consensus trajectories that drive the team to a consensus attitude $q(t_f)$ while satisfying exclusion, avoidance and norm constraints.

There are two aspects of the problem stated above: the first is a *consensus* problem, wherein it is desired to drive the attitudes to a collective consensus attitude, or to various formation attitudes. For bare consensus, the final consensus is that each spacecraft should eventually point to the average of the initial attitudes. However, *relative offset quaternions* can be applied so the consensus attitude can be a desired formation attitude, e.g. each spacecraft can point at 5° away from each other about the z axis. The second problem is that of *avoidance* constraints. This is also important for the team, because spacecraft usually have appendages, some have thrusters that emit plumes, and some have instruments that can be damaged by blinding celestial objects or by the appendage or plume of a team member.

However, the ordinary consensus protocol was not developed for quaternion dynamics. It violates the non-linearity of quaternion kinematics and the quaternion norm preserving requirement. Moreover, the ordinary consensus algorithm also does not incorporate collision avoidance in *adversarial* situations; this is a Q-CAC problem. Thus, in this paper, we present aspects of our previous works [7–9, 16], where we combined consensus theory with constrained optimization to solve the problems stated above. We cast the problems as a *semidefinite program* (SDP), which is augmented with some convex quadratic constraints written as *linear matrix inequalities* (LMI).

We present a quaternion consensus protocol that computes a consensus attitude trajectory each time step, and a Q-CAC optimization procedure, which decides whether it is safe to follow the computed attitude trajectory or not. When generated trajectories are unsafe, it

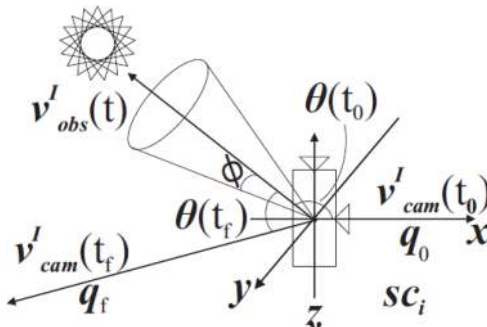


Figure 1. Constrained attitude control problem for a single-spacecraft single-exclusion scenario.

computes a new set of quaternion vectors that avoid collision and the cycle repeats until consensus is achieved.

To understand the avoidance aspect, we begin with a simpler illustration of the spacecraft Q-CAC problem with a single spacecraft and a single obstacle (exclusion) vector, as shown in **Figure 1**.

Let SC_i denote spacecraft i , and $v_{cam_i}^I(t)$ denote the unit camera vector in $\mathcal{F}_{SC_i}^I$ corresponding to the SC_i 's attitude q^i (see **Table 1** for definitions). Also, let $v_{obs_i}^I(t)$ be the attitude quaternion representing the obstacle to be avoided (e.g. the Sun, as shown in **Figure 1**). It is desired that the time evolution of camera vector $v_{cam_i}^I(t_0)$ to $v_{cam_i}^I(t_f)$ should avoid $v_{obs_i}^I(t)$ always, while maintaining a minimum angular separation of \emptyset . The requirement can therefore be stated as

$$\theta(t) \geq \emptyset \tag{1}$$

or

$$v_{cam_i}^I(t)^T v_{obs_i}^I(t) \leq \cos \emptyset, \tag{2}$$

$$\forall t \in [t_0, t_f]$$

The constraint is *non-convex* and *quadratic* and should be *convexified* for it to be represented as a LMI. The convexification was provided in [4], using the quaternion attitude constraints formulation developed in [3] for a single-spacecraft single-obstacle scenario. For that solution, v_{obs}^I was static, $v_{cam_i}^I(t)$ was evolving, and both vectors were in the same coordinate frame. This makes it incomplete for practical implementation because, in reality the obstacle and spacecraft are in different coordinate frames.

In [7–9, 16], we extended the previous avoidance solution to multiple spacecraft. Then we developed a consensus theory of quaternions and appended the new avoidance protocols. We further solved the problem for spacecraft and dynamic obstacles in different coordinate frames to make the solutions more suitable for practical implementation. Next, we present the basic mathematical preliminaries.

3. Mathematical background

In this section, we consider the two basic mathematical theories relevant to this chapter.

3.1. Quaternion-based rotational dynamics

It is convenient to use unit quaternions to represent the attitude of a rigid body rotating in three-dimensional space (such as spacecraft or satellite) because quaternions are not susceptible to the problems of singularities inherent in using Euler angles [17].

The quaternion is a four-element vector

$$q = [q_1 \ q_2 \ q_3 | q_4]^T. \quad (3)$$

Here, $[q_1 \ q_2 \ q_3]^T$ is a vector representing the axis of rotation in the Cartesian (x, y, z) coordinates and q_4 is a scalar representing the angle of rotation, of the quaternion. The difference between two quaternions q^1 and q^2 can be represented in multiplication terms as

$$\begin{aligned} q^d &= q^1 \odot q^{-2} = q^1 \odot [-q_1^2 \ -q_2^2 \ -q_3^2 \ -q_4^2]^T \\ &= Q^2 q^1, \end{aligned} \quad (4)$$

where q^{-2} is the conjugate of q^2 and \odot is defined in **Table 1**. Q^2 is defined as

$$Q^i = \begin{bmatrix} q_4^i & q_3^i & -q_2^i & -q_1^i \\ -q_3^i & q_4^i & q_1^i & -q_2^i \\ q_2^i & -q_1^i & q_4^i & -q_3^i \\ q_1^i & q_2^i & q_3^i & q_4^i \end{bmatrix} \quad (5)$$

It follows that the transformation of q^1 to q^2 was achieved by the rotation quaternion q^d .

The rotational dynamics for the i^{th} quaternion is

$$\dot{q}^i = \frac{1}{2} \Omega^i q^i = \frac{1}{2} \Pi^i \omega^i, \quad (6)$$

where

$$\Omega^i = \begin{bmatrix} 0 & \omega_3^i & -\omega_2^i & \omega_1^i \\ -\omega_3^i & 0 & \omega_1^i & \omega_2^i \\ \omega_2^i & -\omega_1^i & 0 & \omega_3^i \\ -\omega_1^i & -\omega_2^i & -\omega_3^i & 0 \end{bmatrix} \quad (7)$$

$$\Pi^i = \begin{bmatrix} -q_4^i & q_3^i & -q_2^i \\ -q_3^i & -q_4^i & q_1^i \\ q_2^i & -q_1^i & -q_4^i \\ q_1^i & q_2^i & q_3^i \end{bmatrix} \quad (8)$$

Euler's first-order discretization of Eq. (6) gives

$$q^i(k+1) = q^i(k) + \frac{\Delta t}{2} \Pi^i(k) \omega^i(k). \quad (9)$$

The dynamics of the rotational velocity ω^i is

$$\begin{aligned}
 \begin{bmatrix} \dot{\omega}_1^i \\ \dot{\omega}_2^i \\ \dot{\omega}_3^i \end{bmatrix} &= \begin{bmatrix} ((J_2^i - J_3^i)\omega_2^i\omega_3^i + \tau_1^i)/J_1^i \\ ((J_3^i - J_1^i)\omega_3^i\omega_1^i + \tau_2^i)/J_2^i \\ ((J_1^i - J_2^i)\omega_1^i\omega_2^i + \tau_3^i)/J_3^i \end{bmatrix} \\
 &= \underbrace{\begin{bmatrix} 0 & \frac{J_2^i}{J_1^i}\omega_3^i & -\frac{J_3^i}{J_1^i}\omega_2^i \\ \frac{J_3^i}{J_2^i}\omega_3^i & 0 & -\frac{J_1^i}{J_2^i}\omega_1^i \\ \frac{J_1^i}{J_3^i}\omega_2^i & -\frac{J_2^i}{J_3^i}\omega_1^i & 0 \end{bmatrix}}_{\gamma^i} \begin{bmatrix} \omega_1^i \\ \omega_2^i \\ \omega_3^i \end{bmatrix} + \underbrace{\begin{bmatrix} 1/J_1^i & 0 & 0 \\ 0 & 1/J_2^i & 0 \\ 0 & 0 & 1/J_3^i \end{bmatrix}}_{j^i} \begin{bmatrix} \tau_1^i \\ \tau_2^i \\ \tau_3^i \end{bmatrix} \quad (10)
 \end{aligned}$$

Euler’s first-order discretization of Eq. (10) is

$$\omega^i(k+1) = (\mathbf{I}_3 + \Delta t \gamma^i(k))\omega^i(k) + \Delta t j^i \tau^i(k), \quad (11)$$

where J_j^i is the moment of inertia, ω_j^i is the rotational velocity and τ_j^i is the control torque, along the three principal axes $j=1, 2, 3$, for the i^{th} rigid body. Combining Eqs. (9) and (11) in stacked vector form yields

$$\underbrace{\begin{bmatrix} \tau^i(k) \\ \omega^i(k+1) \\ q^i(k+1) \end{bmatrix}}_{\Xi(k+1)} = \underbrace{\begin{bmatrix} \Xi^i(k) & \Psi^i(k) \\ \mathbf{I}_3 + \Delta t \gamma^i(k) + \Delta t j^i \Xi^i(k) & \Delta t j^i \Psi^i(k) \\ \frac{\Delta t}{2} \Pi^i(k) & \mathbf{I}_4 \end{bmatrix}}_{F(k)} \underbrace{\begin{bmatrix} \omega^i(k) \\ q^i(k) \end{bmatrix}}_{\Xi(k)} \quad (12)$$

It is the task of controller synthesis to determine the Ξ^i and Ψ^i to obtain the torque τ^i that stabilizes the system.

3.2. Basic consensus theory

The *Consensus*-based algorithms are distributed protocols based on *communication graphs*, which can drive the states of a team of communicating agents to an agreed state or a common state. The agents (or vehicles) i ($i=1, \dots, n$) are represented by vertices of the graph and the edges of the graph are the communication links between them. Denote the state of a vehicle i as x^i ; \mathbf{x} is the stacked vector of the states all vehicles in the team, then for systems modeled by first-order dynamics, the following first-order consensus protocol (or similar protocols) have been proposed, e.g. [18, 19]

$$\dot{\mathbf{x}}(t) = -\mathbf{L}(\mathbf{x}(t) - \mathbf{x}^{off}). \quad (13)$$

When $\|x^i - x^j\| \rightarrow (x^{ij})^{off}$ as $t \rightarrow \infty$, $\forall i \neq j$ then consensus has been achieved. A more comprehensive presentation of the mathematical basis of consensus (including graph theory), can be found in [16].

However, the basic consensus protocol Eq. (13) cannot admit quaternions directly. Thus, to extend Eq. (13) to attitude quaternions, the following consensus protocol for quaternions was proposed in [7]

$$\dot{\mathbf{q}}(t) = -\mathbf{P}(t)(\mathbf{q}(t) \ominus \mathbf{q}^{-off}), \quad (14)$$

where $\mathbf{P}(t)$ is a Laplacian-like matrix and $\mathbf{q}(t) = [q^1(t), q^2(t) \cdots q^n(t)]^T$. More analysis of $\mathbf{P}(t)$ follows in the next sections.

4. Solutions

We present solutions to the problem statement in Section 2 [7–9, 16]. The solution involves four steps: (1) synthesis of consensus attitudes for multiple spacecraft; (2) formulation of Q-CAC in different coordinate frames; (3) determining obstacle vectors in different coordinate frames; (4) integration for consensus based Q-CAC.

4.1. Synthesis of consensus attitudes for multiple spacecraft

To develop consensus for quaternions, we adopt an optimization approach. The Laplacian-like stochastic matrix $\mathbf{P}(t)$ in Eq. (14) is synthesized (by an optimization process) at each time step to drive $\mathbf{q}(t)$ to consensus while satisfying quaternion kinematics. The components of $\mathbf{P}(t)$ are

$$\mathbf{P}(t) = \underbrace{\begin{bmatrix} \Lambda^1(t) & \cdots & 0 \\ \vdots & \ddots & \vdots \\ 0 & \cdots & \Lambda^n(t) \end{bmatrix}}_{\Lambda(t)} \underbrace{\begin{bmatrix} l_{11}\mathbf{I}_4 & \cdots & l_{1n}\mathbf{I}_4 \\ \vdots & \ddots & \vdots \\ l_{n1}\mathbf{I}_4 & \cdots & l_{nn}\mathbf{I}_4 \end{bmatrix}}_{\Gamma = \mathbf{L} \otimes \mathbf{I}_4}, \quad (15)$$

where $\Lambda^i(t) > 0$ is an unknown positive definite optimization matrix variable, whose components are chosen by the optimization process. Matrix Γ is composed of components of the Laplacian $\mathbf{L} = [l_{ij}]$ ($i, j = 1, \dots, n$), which gives $\mathbf{P}(t)$ its Laplacian-like behavior.

We shall now prove the stability of $\mathbf{P}(t)$, i.e. that Eq. (14) does indeed achieve consensus. Note that all the theorems, lemmas and proofs in this section had been presented in [7].

Recall the following standard result on a *matrix pencil* [20].

Theorem 1: For a *symmetric-definite pencil* $\mathbf{A} - \lambda\mathbf{B}$, there exists a nonsingular $S = [s_1, \dots, s_n]$ such that

$$S^T \mathbf{A} S = \text{diag}(a_1, \dots, a_n) = D_A, \quad (16)$$

$$S^T \mathbf{B} S = \text{diag}(b_1, \dots, b_n) = D_B. \quad (17)$$

Moreover, $\mathbf{A}s_i = \lambda_i \mathbf{B}s_i$ for $i = 1, \dots, n$, where $\lambda_i = a_i/b_i$.

Lemma 1: For any time t , the eigenvalues of $\mathbf{P}(t)$ are $\gamma_i \eta_i(t)$. Here, γ_i are the eigenvalues of Γ and $\eta_i(t)$ the eigenvalues of $\Lambda(t)$. It can therefore be observed that $\mathbf{P}(t)$ has only four zero eigenvalues, the rest of its eigenvalues are strictly positive.

Proof: To find the eigenvalues of $\mathbf{P}(t)$, consider a scalar λ such that for some nonzero vector s

$$\Gamma s = \lambda \Lambda^{-1}(t) s. \tag{18}$$

Eq. (18) defines a *symmetric-definite generalized eigenvalue problem* (SDGEP), where $\Gamma - \lambda \Lambda^{-1}(t)$ defines a matrix pencil. Theorem 1 therefore immediately implies that the eigenvalues of $\mathbf{P}(t)$ are $\gamma_i \eta_i(t)$. One can also easily observe that due to the property of the Laplacian matrix \mathbf{L} , $\mathbf{P}(t)$ has positive eigenvalues except for four eigenvalues. This proves the claim.

Theorem 2: The time-varying system Eq. (14) achieves consensus.

Proof: for simplicity, let us assume that there are no offsets, i.e. $\mathbf{q}^{off} = 0$ (or $(q^{off})^i = [0 \ 0 \ 0 \ 1]^T \forall i$). Note, when \mathbf{q} has entered the *consensus space* $\mathcal{C} = \{\mathbf{q} | q^1 = q^2 = \dots = q^n\}$, then $\dot{\mathbf{q}} = 0$. \mathcal{C} is the *nullspace* of $\mathbf{P}(t)$, i.e. the set of all \mathbf{q} such that $\mathbf{P}(t)\mathbf{q} = 0$. Therefore, once \mathbf{q} enters \mathcal{C} it stays there.

Suppose that \mathbf{q} has not entered \mathcal{C} , then consider a Lyapunov candidate function $V = \mathbf{q}^T \Gamma \mathbf{q}$; $V > 0$ unless $\mathbf{q} \in \mathcal{C}$. Then,

$$\begin{aligned} \dot{V} &= \dot{\mathbf{q}}^T \Gamma \dot{\mathbf{q}} + \dot{\mathbf{q}}^T \Gamma \mathbf{q} \\ &= -\mathbf{q}^T \Gamma \mathbf{P}(t) \mathbf{q} - \mathbf{q}^T \mathbf{P}(t)^T \Gamma \mathbf{q} \\ &= -\mathbf{q}^T \Gamma \Lambda(t) \Gamma \mathbf{q} - \mathbf{q}^T \Gamma \Lambda(t) \Gamma \mathbf{q} \\ &= -2\mathbf{q}^T \Gamma \Lambda(t) \Gamma \mathbf{q} \\ &= -2z^T \Lambda(t) z, \end{aligned} \tag{19}$$

where $z = \Gamma \mathbf{q} \neq 0$ for $\mathbf{q} \notin \mathcal{C}$. This implies that \mathbf{q} approaches a point in \mathcal{C} as $t \rightarrow \infty$, which proves the claim. Eq. (19) is true as long as \mathbf{L} is nonempty, i.e. if some vehicles can sense, see, or communicate with each other all the time.

4.2. Formulation of Q-CAC in different coordinate frames

Any rigid appendage attached to the body of the i^{th} spacecraft, e.g. a camera, whose pointing direction is $v_{cam_i}^I$ in inertial frame, can be transformed to the spacecraft fixed body frame by the rotation

$$v_{cam_i}^B(t) = \mathcal{R}_i^{-1}(t) v_{cam_i}^I(t), \tag{20}$$

where

$$\mathcal{R}_i(t) = \left((2q_4^i(t))^2 - 1 \right) \mathbf{I}_3 + 2\bar{q}^i(t) \bar{q}^i(t)^T - 2q_4^i(t) \bar{q}^i(t)^\times \tag{21}$$

is the rotation matrix corresponding to the $q^i(t)$ at time t ; $\bar{q}^i(t)^\times$ is the *antisymmetric matrix* [21].

For simplicity let us consider a single SC_i with a single camera, $v_{cam_i}^I$, and m (possibly, time-varying) obstacles, $v_{obs_i,j}^I$ ($j = 1, \dots, m$), defined in $\mathcal{F}_{SC_i}^I$ to be avoided by $v_{cam_i}^I$ when SC_i is re-orientating. Then according to [3], the resulting attitude constraint of Eq. (2) can be written as

$$q^i(t)^T \tilde{A}_j^i(t) q^i(t) \leq 0. \quad (22)$$

Its LMI equivalent according to [4] is

$$\begin{bmatrix} \mu & q^i(t)^T \\ q^i(t) & (\mu \mathbf{I}_4 + \tilde{A}_j^i(t))^{-1} \end{bmatrix} \geq 0. \quad (23)$$

In Eq. (23), μ is chosen to ensure $\mu \mathbf{I}_4 + \tilde{A}_j^i(t)$ is positive definite, and

$$\tilde{A}_j^i(t) = \begin{bmatrix} A_j(t) & b_j(t) \\ b_j(t)^T & d_j(t) \end{bmatrix} \in \mathbb{R}^{4 \times 4}, \quad (24)$$

where

$$A_j(t) = v_{cam_i}^B(t) v_{obs_i,j}^I(t)^T + v_{obs_i,j}^I(t) v_{cam_i}^B(t)^T - (v_{cam_i}^B(t)^T v_{obs_i,j}^I(t) + \cos \theta) \mathbf{I}_3, \quad (25)$$

$$b_j(t) = -v_{cam_i}^B(t) \times v_{obs_i,j}^I(t), \quad (26)$$

$$d_j(t) = v_{cam_i}^B(t)^T v_{obs_i,j}^I(t), \quad (27)$$

for $j = 1, \dots, m$.

Eq. (22) defines the set of attitude quaternions $q^i(t)$ to satisfy the constraint $v_{cam_i}^I(t)^T v_{obs_i,j}^I(t) \geq \theta \forall t \in [t_0, t_f]$, so it is used to find a collision-free $v_{cam_i}^I(t)$. However, in practical situations, another SC (SC_j) can be near SC_i , then another obstacle vector $v_{obs_j}^I(t)$ (e.g. a thruster vector emanating from SC_j) defined in $\mathcal{F}_{SC_j}^I$ should be avoided by SC_i . To address such a practical issue, we present a mechanism to calculate $v_{obs_i,j}^I$ (defined in $\mathcal{F}_{SC_i}^I$) corresponding to $v_{obs_j}^I$ (defined in $\mathcal{F}_{SC_j}^I$) ($v_{obs_i,j}^I$ means the obstacle vector originated from the rotating frame of SC_j but defined in $\mathcal{F}_{SC_i}^I$). Essentially, the mechanism determines the intersection point of $v_{obs_j}^I(t)$ with the sphere of radius r , centered on SC_i . If such an intersection exists, it defines $v_{obs_i,j}^I$ which can be used to define an attitude constraint represented as Eq. (22) to be avoided by SC_i .

Figure 2 illustrates the scenario. SC_1 and SC_2 are in their different coordinate frames relative to Earth. A thruster attached to SC_1 body frame is at $v_{obs_1}^I$, while the circles around SC_1 and SC_2 are spheres representing the coordinate frames from which their attitude evolves. If both spacecraft are close enough, then vector $v_{obs_1}^I$ may intersect a point on the sphere of SC_2 ,

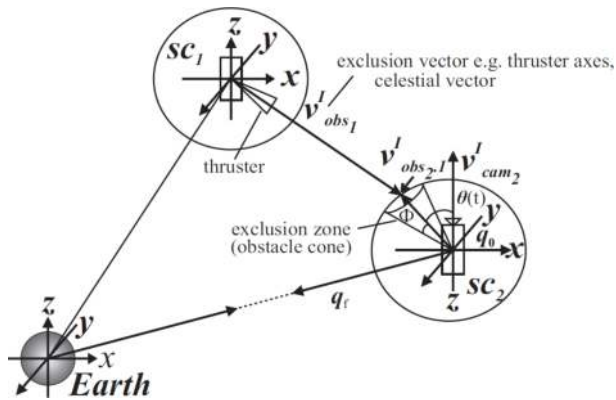


Figure 2. Q-CAC problem in different frames.

whereby the intersection defines $v^I_{obs_{2,1}}$ in the frame of SC_2 . The requirement is that as SC_2 changes its attitude from q_0 to q_f , $v^I_{cam_2}$ must avoid the cone created around $v^I_{obs_{2,1}} \forall t \in [t_0, t_f]$.

4.3. Determination of obstacle vectors in different coordinate frames

Given SC_i in $\mathcal{F}^I_{SC_i}$ and SC_j in $\mathcal{F}^I_{SC_j}$, with emanating vectors, one can easily determine an intersection between a vector emanating from $\mathcal{F}^I_{SC_j}$ with the sphere centered on $\mathcal{F}^I_{SC_i}$ by using onboard sensors, or by application of computational geometry. Given a line segment originating at p_1 and terminating at p_2 , a point $p = [p_x \ p_y \ p_z]^T$ on $[p_1, p_2]$ can be tested for intersection with a sphere centered at p_3 with radius r [22]. Thus, for any $v^I_{obs_j}(t)$ in $\mathcal{F}^I_{SC_j}$, if an intersection point $p(t)$ exists at time t with the sphere centered on $\mathcal{F}^I_{SC_i}$ with radius r , then $v^I_{obs_j}(t) = p(t)$; otherwise, one can set $v^I_{obs_j}(t) = -v^I_{cam_i}(t)$, to show that no constraints violation has occurred. The value of r will therefore depend on the application at hand, but must be proportional to the urgency of avoiding obstacle vectors originating from other spacecraft.

The above formulation effectively decentralizes the problem. Therefore, each spacecraft can solve the problem by communicating with its neighbors and/or using its own sensors. Euler first order discretization of Eq. (14) is

$$q_{k+1} = q_k + \Delta t \dot{q}_k = q_k - \Delta t P(t) q_k. \tag{28}$$

The decentralized dynamics for any SC_i is therefore

$$q^i_{k+1} = q^i_k - \Delta t \underbrace{\left[y \Lambda_1^i(t) - \Lambda_2^i(t) \cdots - \Lambda_y^i(t) \right]}_{P^i(t)} \left[q^T_1(t) \ q^T_2(t) \cdots q^T_y(t) \right]^T, \tag{29}$$

where $q_1^T(t)$ $q_2^T(t)$... $q_y^T(t)$ are the quaternions of the y other neighboring SC, which SC_i can communicate with at time t . Moreover, since we are going to apply consensus quaternion protocol Eq. (29), norm constraints must be enforced as follows:

$$q_k^i T(q_{k+1}^i - q_k^i) = 0 \quad (30)$$

Eq. (30) is the discrete time version of $q^i(t)^T \dot{q}^i(t) = 0$ or $\mathbf{q}(t)^T \dot{\mathbf{q}}(t) = 0$. This guarantees that $q^i(t)^T q^i(t) = 1$ or $\mathbf{q}(t)^T \mathbf{q}(t) = n$ for SC, iff $\|q^i(0)\| = 1 \forall i$.

4.4. Integration for consensus based Q-CAC

Using semidefinite programming, the solutions presented previously be cast as an optimization problem, augmented with a set of LMI constraints, and solved for optimal consensus quaternion trajectories. We consider the algorithm in discrete time. Given the initial attitude $q^i(0)$ of SC_{i^v} ($i=1, \dots, n$), find a sequence of consensus quaternion trajectories that satisfies the following constraints:

$$q_{k+1}^i = q_k^i - \Delta t \mathbf{P}^i(t) q_k^i \quad \text{quaternion consensus dynamics constraint} \quad (31)$$

$$q_k^i T(q_{k+1}^i - q_k^i) = 0, \quad \text{norm constraint} \quad (32)$$

$$\begin{bmatrix} \mu & q^i(t)^T \\ q^i(t) & (\mu \mathbf{I}_4 + \tilde{A}_j^i(t))^{-1} \end{bmatrix} \geq 0 \quad \text{exclusion constraints} \quad (33)$$

Once the next safe quaternion trajectory q_{safe}^i has been determined, the control torque τ^i and angular velocity ω^i to rotate the SC_i optimally to q_{safe}^i can be determined by using the normal quaternion dynamics Eq. (12).

5. Simulation results

Due to limitation of space, we present three results for attitude multi-path planning in different coordinate frames. More results can be found in [7, 8, 16].

5.1. Dynamic avoidance in different coordinate frames without consensus

In this experiment, SC_1 and SC_2 are attempting a reconfiguration to Earth (either changing orientation to Earth or pointing an instrument to Earth). The initial quaternions of SC_1 and SC_2 are $q_0^1 = q_0^2 = [0 \ 0 \ 0 \ 1]^T$. The desired final quaternions are

$$\begin{aligned} q_f^1 &= [0.2269 \ 0.0421 \ 0.9567 \ 0.1776]^T \\ q_f^2 &= [0 \ 0 \ 0.9903 \ 0.1387]^T \end{aligned} \quad (34)$$

Three thrusters of SC_1 in $\mathcal{F}_{SC_1}^B$ are

$$\begin{aligned}
 v_{obs1,1}^B &= [-0.2132 \quad -0.0181 \quad 0.9768]^T \\
 v_{obs1,2}^B &= [0.314 \quad 0.283 \quad -0.906]^T \\
 v_{obs1,3}^B &= [-0.112 \quad -0.133 \quad -0.985]^T
 \end{aligned}
 \tag{35}$$

A single thruster of SC_2 in $\mathcal{F}_{SC_2}^B$ is at

$$v_{obs2}^B = [0.02981 \quad 0.0819 \quad 0.9962]^T
 \tag{36}$$

We want v_{obs2}^I to avoid $v_{obs1,1}^I$ by 50° , and avoid $v_{obs1,2}^I$ and $v_{obs1,3}^I$ by 30° while both are maneuvering to their desired final attitudes. **Figure 3(a)** shows the avoidance between thrusters of SC_1 and SC_2 during reorientation to Earth: SC_2 cannot reconfigure to the desired q_f^2 due to the avoidance constraints. Note that $v_{obs2,1}^I, v_{obs2,2}^I, v_{obs2,3}^I$ are the points of intersections of $v_{obs1,1}^I, v_{obs1,2}^I, v_{obs1,3}^I$ with SC_2 . **Figure 3(b)** satisfaction of avoidance constraints: the sudden jumps to and from -1 indicate times when any of $v_{obs1,1}^I, v_{obs1,2}^I, v_{obs1,3}^I$ lost intersection with the sphere of SC_2 and therefore was replaced with $-v_{obs1,i}^I, i = 1, \dots, 3$.

This experiment demonstrates that when both constraints are in conflict the avoidance constraint is superior to the desired final quaternion constraint. As seen from (a), SC_2 cannot reconfigure exactly to the desired q_f^2 due to the satisfaction of the avoidance constraints. To resolve this, it is necessary to change either the position of SC_2 or SC_1 .

5.2. Consensus-based dynamic avoidance in different coordinate frames

In this experiment, SC_1, SC_2 , and SC_3 will maneuver to a consensus attitude. The initial positions are

$$\begin{aligned}
 \mathcal{F}_{SC_1}^I &= [-2 \quad 0 \quad 2]^T \\
 \mathcal{F}_{SC_2}^I &= [0.5 \quad 0 \quad 2]^T \\
 \mathcal{F}_{SC_3}^I &= [3 \quad 0 \quad 2]^T
 \end{aligned}
 \tag{37}$$

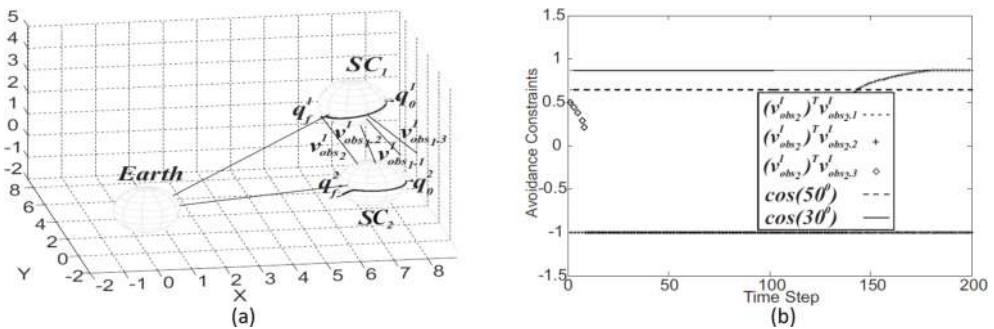


Figure 3. Reconfiguration of two spacecraft with avoidance in different coordinate frames: (a) the trajectories, (b) the avoidance graph.

A set of initial quaternions were randomly generated, with the following data:

$$\begin{aligned} q_0^1 &= [-0.5101 \ 0.6112 \ -0.3187 \ -0.5145]^T \\ q_0^2 &= [-0.9369 \ 0.2704 \ -0.1836 \ -0.124]^T \\ q_0^3 &= [0.1448 \ -0.1151 \ 0.1203 \ 0.9753]^T \end{aligned} \quad (38)$$

In the direction of the initial attitude q_0^i of each SC_i , a sensitive instrument $v_{cam_i}^I$ is attached. Also, each SC_i has a thruster pointing to the opposite of q_0^i . It is desired that $v_{cam_i}^I$ avoids the thruster plumes emanating from each of the two other SC by 30° during the entire period of the maneuvers. From the generated initial quaternions, there is possibility of intersection of the thrusters of SC_1 and SC_3 , with SC_2 , and the thruster of SC_2 may damage SC_1 or SC_3 at any time k . **Figure 4(a)** shows the solution trajectories; (b) shows the avoidance graph, which shows that constraints are not violated; (c) shows the consensus graph. The final consensus quaternion is $q_f = [-0.8167 \ 0.4807 \ -0.2396 \ 0.2112]^T$. This is the normalized average of the initial attitude quaternions, which proves that consensus is achieved.

5.3. Consensus-based attitude formation acquisition with avoidance

To test the capability of the consensus algorithm in formation acquisition, SC_1 , SC_2 , and SC_3 will maneuver to a consensus formation attitude. Relative offset quaternions were defined to enable the sensitive instruments to point at 30° offsets from each other about the z-axis. The previous set of initial data for q_0^i and $\mathcal{F}_{SC_i}^I$ were used. The relative offsets are

$$\begin{aligned} q_1^{off} &= [0 \ 0 \ 0 \ 1]^T \\ q_2^{off} &= [0 \ 0 \ 0.2588 \ 0.9659]^T \\ q_3^{off} &= [0 \ 0 \ 0.5 \ 0.866]^T \end{aligned} \quad (39)$$

Like the previous experiment, we want the sensitive instruments to avoid the thruster plumes emanating from each of the two other SC by an angle of 30° . The trajectories are shown in **Figure 5(a)** and (b) shows the avoidance graph; no constraints are violated, and (c) shows the consensus graph. The final consensus quaternions are

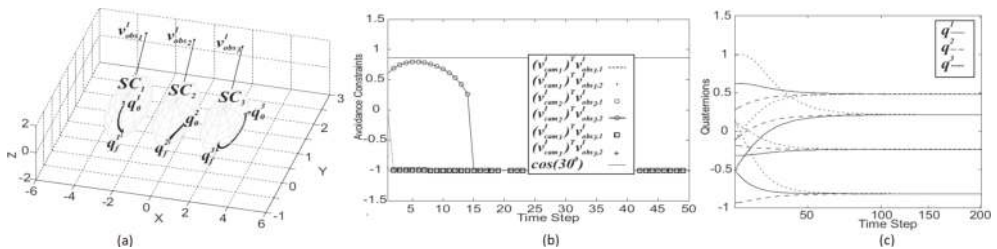


Figure 4. Consensus-based dynamic avoidance in different coordinate frames. (a) Reorientation to consensus attitude with intervehicle thruster plume avoidance, (b) avoidance constraints graph, (c) attitude consensus graph.

$$\begin{aligned} q_f^1 &= [-0.6926 \ 0.6468 \ -0.2798 \ 0.1541]^T \\ q_f^2 &= [-0.8364 \ 0.4455 \ -0.2303 \ 0.2212]^T \\ q_f^3 &= [-0.9232 \ 0.2138 \ -0.1652 \ 0.2733]^T \end{aligned} \quad (40)$$

The differences of these quaternions are 30° apart about the same axis.

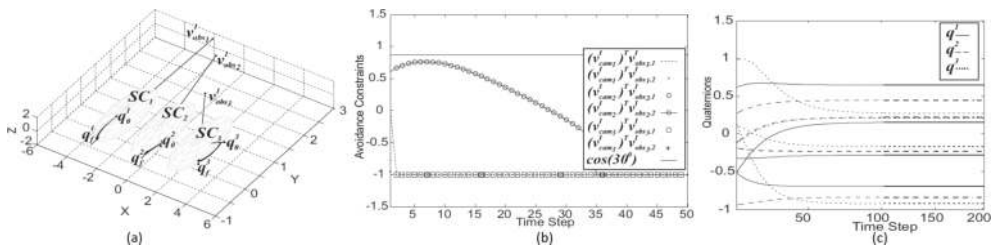


Figure 5. Consensus-based attitude formation acquisition with avoidance. (a) Reorientation to consensus formation attitude with intervehicle thruster plume avoidance, (b) avoidance constraints graph, (c) attitude consensus graph.

6. Conclusion

We presented a solution, which we previously developed, to the problem of attitude path planning for multiple spacecraft with avoidance of exclusion zones, by combining consensus theory and Q-CAC optimization theory. Using the solutions, a team of spacecraft can point to the same direction, or to various formation patterns, while they avoid an arbitrary number of attitude obstacles or exclusion zones in any coordinate frames. We also provided the proof of stability of the Laplacian-like matrix used for the attitude synchronization. Simulation results demonstrated the effectiveness of the algorithm. Current work is underway to implement the algorithms using rotorcraft.

Author details

Innocent Okoloko

Address all correspondence to: okoloko@ieee.org

Department of Electrical Engineering, Universidad de Ingenieria y Tecnologia, Lima, Peru

References

- [1] Blackwood G, Lay O, Deininger B, Gudim M, Ahmed A, Duren R, Noeckerb C, Barden B. The StarLight mission: A formation-flying stellar interferometer. In: SPIE 4852,

- Interferometry in Space; 22 August; Waikoloa, Hawaii. Bellingham WA, USA: SPIE Digital Library; 2002. DOI: 10.1117/12.460942
- [2] Beichman CA. NASA's Terrestrial Planet Finder. In: Darwin and Astronomy: The Infrared Space Interferometer; 17-19 November; Stockholm, Sweden. The Netherlands: Noordwijk; 2000. pp. 29-30. DOI: ISSN/ISBN: 03796566
- [3] Ahmed A, Alexander J, Boussalis D, Breckenridge W, Macala G, Mesbahi M, Martin MS, Singh G, Wong E. Cassini Control Analysis Book. Pasadena, CA: Jet Propulsion Laboratory, CALTECH Technical Report; 1998. NA p. DOI: NA
- [4] Kim Y, Mesbahi M. Quadratically constrained attitude control via semidefinite programming. *IEEE Transactions on Automatic Control*. 2004;**49**:731-735. DOI: 10.1109/TAC.2004.825959
- [5] Wen JT, Kreutz-Delgado K. The attitude control problem. *IEEE Transactions on Automatic Control*. 1991;**36**(10):1148-1162. DOI: 10.1109/9.90228
- [6] Kim Y, Mesbahi M, Singh G, Hadaegh FY. On the convex parameterization of constrained spacecraft reorientation. *IEEE Transactions on Aerospace and Electronic Systems*. 2010;**46**(3):1097-1109. DOI: 10.1109/TAES.2010.5545176
- [7] Okoloko I, Kim Y. Distributed constrained attitude and position control using graph Laplacians. In: ASME Dynamic Systems and Control Conference; 13-15 September; Cambridge, Massachusetts. NY, USA: ASME; 2010. pp. 377-383. DOI: 10.1115/DSCC2010-4036
- [8] Okoloko I, Kim Y. Attitude synchronization of multiple spacecraft with cone avoidance constraints. In: IEEE Aerospace Conference; 3-10 March; Big Sky, Montana. NY, USA: IEEEExplore; 2012. pp. 1-10. DOI: 10.1109/AERO.2012.6187119
- [9] Okoloko I, Kim Y. Attitude synchronization of multiple spacecraft with cone avoidance constraints. *Systems & Control Letters*. 2014;**69**:73-79. DOI: 10.1016/j.sysconle.2014.04.008
- [10] Bullo F, Murray RM, Sarti A. Control on the sphere and reduced attitude stabilization. In: IFAC Symposium on Nonlinear Control Systems; 25-28 June; Tahoe City, CA. Atlanta GA, USA: Elsevier; 1995. pp. 495-501. DOI: 10.1016/S1474-6670(17)46878-9
- [11] Fax AJ. Optimal and cooperative control of vehicle formations [thesis]. Pasadena, CA: PhD Thesis, CALTECH; 2002. 135 p. Available from: thesis.library.caltech.edu/4230/1/Fax_ja_2002.pdf
- [12] Ren W. Distributed attitude alignment in spacecraft formation flying. *International Journal of Adaptive Control and Signal Processing*. 2006;**21**(2-3):95-113. DOI: 10.1002/acs.916
- [13] Dimarogonas DV, Tsiotras P, Kyriakopoulos KJ. Leader-follower cooperative attitude control of multiple rigid bodies. *Systems and Control Letters*. 2009;**58**(6):429-435. DOI: 10.1016/j.sysconle.2009.02.002

- [14] Sturm JF. Using SeDuMi 1.02, a Matlab toolbox for optimization over symmetric cones. *Optimization Methods and Software*. 1998;**11**(12):625-653. DOI: 10.1080/10556789908805766
- [15] Lofberg J. Yalmip: A toolbox for modelling and optimization in Matlab. In: *IEEE CACSD Conference*; 2-4 Sept.; Taipei, Taiwan. NY, USA: IEEEExplore; 2004. pp. 284-289. DOI: 10.1109/CACSD.2004.1393890
- [16] Okoloko I. Multi-path planning and multi-body constrained attitude control [dissertation]. Stellenbosch, South Africa: PhD Thesis, Stellenbosch University; 2012. 185 p. Available from: <http://hdl.handle.net/10019.1/71905>
- [17] Kuipers JB. *Quaternions and Rotation Sequences: A Primer with Applications to Orbits, Aerospace and Virtual Reality*. 1st ed. Princeton, NJ: Princeton University Press; 2002. 371 p. ISBN: 13: 978-0691102986
- [18] Peng L, Zhao Y, Tian B, Zhang J, Bing-Hong W, Hai-Tao Z, Zhou T. Consensus of self-driven agents with avoidance of collisions. *Physical Review*. 2009;**79**(E):026113. DOI: 10.1103/PhysRevE.79.026113. Available from: <https://journals.aps.org/pre/abstract/10.1103/PhysRevE.79.026113>
- [19] Olfati-Saber R. Flocking for multi-agent dynamic systems: Algorithms and theory. *IEEE Transactions on Automatic Control*. 2006;**51**(3):401-420. DOI: 10.1109/TAC.2005.864190
- [20] Golub GH, Van Loan CF. *Matrix Computations*. 3rd ed. Baltimore, MD: Johns Hopkins University Press; 1996. 699 p. ISBN: 13: 978-0801854149
- [21] Hughes PC. *Spacecraft Attitude Dynamics*. 2nd ed. Mineola, NY: Dover Publications Inc; 2004. 592 p. ISBN: 13: 9780486439259
- [22] Eberly DH. *3D Game Engine Design: A Practical Approach to Real-Time Computer Graphics*. 2nd ed. London, UK: Taylor & Francis; 2012. 1015 p. DOI: ISBN: 978-0-12-229063-3

